邓锡铭

研究论文集

COLLECTION OF THESES

1961-2000

中卷

中国科学院
中国工程物理研究院
高功率激光物理联合实验室

邓锡铭

研究论文集

COLLECTION OF THESES

1961-2000

中卷

中国科学院
中国工程物理研究院
高功率激光物理联合实验室

目　　录

上　　册

中　册

下　册

EVIDENCE, FROM SPACE RESOLVED SPECTRA, OF $2\omega_0$ HARMONIC GENERATION IN LASER IRRADIATED PLASMA FILAMENTS

Min GU, Weihan TAN, Zunqi LIN, Wenhua CHEN, Yuxia ZHENG, Wenyan YU and Ximing DENG
Shanghai Institute of Optics and Fine Mechanics, Academia Sinica, Shanghai, P.R.China

Received 21 September 1987

Space resolved spectra with both high spectral resolution (~0.2 Å) and spatial resolution (~2 μm) of the second harmonic emission scattered at 90° to the laser axis were observed when both narrow band and broad band laser beams were used in an Al planar target experiment. Analysing many experimental phenomena, we have proved that the second harmonic emission observed at 90° to the laser axis is initiated by laser–plasma-filament interaction and not by planar-wave–plasma interaction. The experiments are, on the whole, in agreement with our theory.

1. Introduction

Two generation mechanics, namely linear conversion and parametric decay, for the second harmonic emission from laser plasma have been studied both experimentally and theoretically [1–13]. In terms of the resonance absorption theory based on the assumption that an obliquely incident planar wave with P polarization travels into a plasma with a linear gradient [1,2,14], it has been shown that the second harmonic emission resulting from the linear conversion is mainly emitted in the mirror-reflected direction of the incident laser. In the normally incident case, the linear conversion of the $2\omega_0$ harmonic emission is very weak because the resonance absorption almost disappears. But, it has been found in ref. [15] that, when a laser beam is normally incident, two-dimensional microphotographs of the second harmonic emission scattered at 90° to the laser axis display many filamentary structures with a length of 125 μm, the transverse scale of which is about 5–15 μm. Unfortunately, no satisfactory physical explanation for this phenomena has been put forward. On the other hand, the time resolved spectra, as well as time and space resolved structures, of the second harmonic emission have been observed at 90° to the laser axis in our experiment [12,13]. The filamentary structures extend to 180 μm along the incident direction, close to the length of filaments [16]. All these phenomena can not be explained by the planar wave interaction theory. Therefore, we have considered [14] a new mechanism for the second harmonic emission from plasma filaments, which shows that when a laser beam interacts with plasma filaments, the $2\omega_0$ harmonic emission caused by the linear conversion is mainly emitted in a direction perpendicular to the laser axis.

In this paper, we present a simple description of the mechanism for the second harmonic emission from plasma filaments [14]. Then, both broad band and narrow band laser beams are used in the prepulse and non-prepulse irradiance, irradiating on an Al planar target normally. The second harmonic space resolved spectra scattered at 90° to the laser axis were thus observed. From these spectra, it has been found that the second harmonic emission with a luminescent length of 180 μm extends outward from the critical surface. In this luminescent region, there exist no spectral shifts. Only in the prepulse case, do some red and blue shifted peaks emerge near the critical surface. By comparing the experimental results in the broad band and narrow band irradiance, the new mechanism for the second harmonic emission from a plasma filament [14] may be proved. The experiments are in general, consistent with the theory.

0 030-4018/88/$03.50

2. The mechanism for the $2\omega_0$ harmonic emission in filaments

In ref. [14], the influence of laser plasma filaments on the linear conversion of the $2\omega_0$ harmonic emission were studied in detail. Considering a filament with both a linear density gradient along the z-direction and a radial density distribution, and assuming that a laser beam travels along the z-direction, one can find that there exists an intense local field of the fundamental wave near the radial resonance point r_0 (when $r=r_0$, the dielectric coefficient is equal to zero), which is called the radial tunnel effect [14]. Thus the characteristics of the second harmonic emission generated by this effect are the following.

(i) If the fundamental wave is symmetric about the z-axis, the intensity of the second harmonic emission is zero in the z-direction, but intense in the direction perpendicular to the incident laser.

(ii) If the fundamental wave is asymmetric about the z-axis, the second harmonic generation is emitted both in the z-direction and in the direction perpendicular to the incident laser. Generally, the intensity in the former case is smaller than that in the latter case and depends on the symmetry of the fundamental wave about the z-axis. The better the symmetry, the smaller the intensity in the z-direction.

(iii) The second emission displays a large luminescent region, extending outward from the critical surface along the z-axis. The luminescent length is of the same order as that of a plasma filament.

(iv) Since the second harmonic emission is caused by the linear conversion, its spectrum shows no red shifts.

3. Experimental setup and results

3.1. Experimental setup

The experiments were carried out at the Six Laser Beam Facility in the Shanghai Institute of Optics and Fine Mechanics. It has been shown in our previous experiments [17] that the laser illumination on the target surface in narrow band irradiance is non-uniform and filaments are easily produced. Conversely, in the broad band irradiance the laser illumination

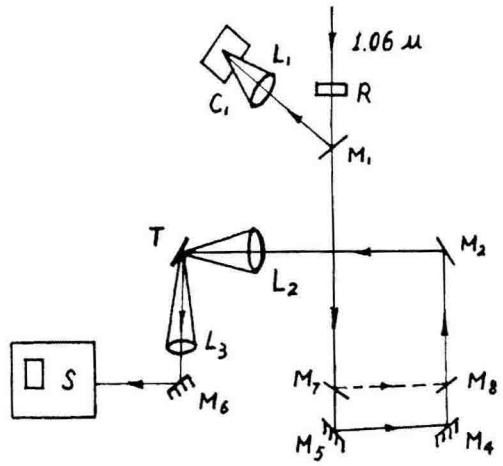

Fig. 1. Experimental setup.

is uniform and it is difficult to initiate the filamentation process. Therefore, the influences of the plasma filament on the second harmonic emission can be studied by adopting the broad band and narrow band lasers. The methods used to generate broad band and narrow band lasers have been described in refs. [17,18]. The broad band laser had a bandwidth of ~ 30 Å while the narrow band laser bandwidth was 0.2 Å. Both broad band and narrow band lasers had an output energy of 0.4–10 J, pulse width 250 ps, and power density $(0.3\text{–}8)\times 10^{14}$ W/cm^2.

The experimental arrangement is shown in fig. 1, where M_1, C_1 and L_1 are sampling mirror, energy calorimeter and focusing lens, respectively, for the measurement of the incident laser energy. Both broad and narrow band incident lasers then passed through a quartz optical rotation plate R with 45° left- or 45° righ-handed rotation, becoming P (horizontally) or S (vertically) polarized with respect to the target plane. Two partly reflecting plates M_7 and M_8 for the wavelength of 1.06 μm were inserted in the path to form a prepulse with a magnitude of 0.1% of the main pulse energy and an arrival time ahead of the main pulse 0.15 ns. The incident laser was focused by an $f/2$ aspherical lens L_2 on an Al planar target surface with an incident angle $\theta=3°$, resulting in the second harmonic emission.

The spectrograph S, with a dispersive power of 16 Å/mm for the wavelength of 0.53 μm, was oriented at 90° to the incident laser, and its slit, the length and width of which are 6 mm × 100 μm, was placed

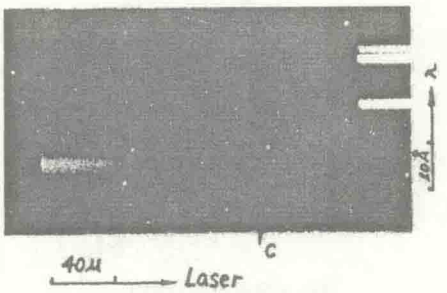

Fig. 2. $2\omega_0$ harmonic space resolved spectrum of irradiation no. 17 with narrow band laser irradiance on an Al planar target and incident angle of 3°, energy 3.0 J, 45° polarization.

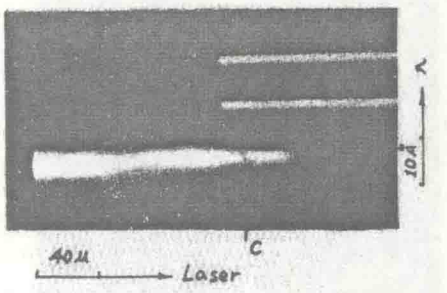

Fig. 3. $2\omega_0$ harmonic space resolved spectrum of irradiation no. 21 with narrow band laser irradiance on an Al planar target and incident angle of 3°, energy 6.5 J, vertical polarization.

in the horizontal direction. By using micro-objective L_3 ($f=100$ μm) and mirror M_6 for the wavelength of 0.53 μm, a sampling window at the target normal, 5 μm × 280 μm, was formed. Thus, we can obtain the second harmonic space resolved spectra produced by plasma filaments with both high spatial resolution (~2 μm) and spectral resolution (~0.2 Å). Some interference filters with central wavelength 0.53 μm and totally reflecting plates for 1.06 μm were set in front of the spectrograph slit, so that one could adjust the signal intensity and cut out the scattered lights.

3.2. Experimental results

The second harmonic space resolved spectra obversed at 90° to the incident laser under the condition of non-prepulse and prepulse irradiance are shown in figs. 2, 3 and 4, respectively, calibrated by spectral lines of Ne atoms. The wavelength of the first Ne spectral line near the $2\omega_0$ harmonic spectra is 5330.78 Å. Analyzing these spectra in detail, one could notice the following features.

3.2.1. Non-prepulse case

(i) The $2\omega_0$ harmonic luminescent length along the incident laser varies with the incident energy. When the incident energy is smaller (about 3 J), the $2\omega_0$ harmonic emission extends outward from a position, 60 μm from the critical surface (see fig. 2, where point c denotes the position of the critical surface). The luminescent length in the detecting range of the spectrograph is about 30–40 μm. If the energy increases further, for example, the incident energy is 7 J, the $2\omega_0$ harmonic luminescent length then becomes 180 μm, extending to the critical surface.

(ii) The central position of the $2\omega_0$ harmonic space resolved spectrum shows no red shifts within the whole luminescent region. The spectral width is about 5.6 Å near the critical surface and 7.2 Å far away from the critical surface.

(iii) In the case of narrow band irradiance, the second harmonic emission was generated not only in the backscattering direction but also in the direction perpendicular to the incident laser even if the incident energy is smaller. However, when a broad band laser irradiates an Al planar target, the second harmonic intensity in the direction perpendicular to the incident laser is too small to be recorded by the spectrograph.

3.2.2. Prepulse case

Some interesting results obtained in the prepulse irradiance are displayed in fig. 4. When a narrow band laser with a prepulse irradiates an Al planar target, the intense second harmonic emission with a luminescent length of 120 μm along the incident laser is still observed in the direction perpendicular to the incident laser. Besides, the central position of the spectrum with a width of 4.8 Å shows no red shifts. Conversely, in the broad band case, only when the incident energy is larger than 10 J (corresponding to a power density of 8×10^{14} W/cm^2), can the second harmonic emission be detected in the direction perpendicular to the incident laser. Comparing figs. 2 and 3 with fig. 4, one can find the following differences near the critical surface.

(i) The $2\omega_0$ harmonic emission is more intense

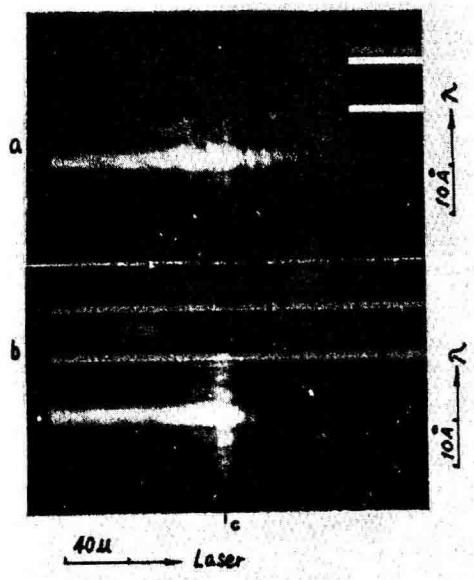

Fig. 4. $2\omega_0$ harmonic space resolved spectra with narrow band laser irradiance on an Al planar target and incident angle of 3°. (a) Irradiation no. 89, 2.9 J, 45° polarization. (b) Irradiation no. 90, 2.5 J, 45° polarization.

near the critical surface than that in the other region.

(ii) There are some fine space fringes with intervals of 8 μm along the incident laser (see fig. 4a).

(iii) From fig. 4, as well as its densitometric traces in fig. 5, it is shown that there are some symmetric red and blue shifted peaks. The interval between peaks is about 3.8 Å.

4. Discussion

The second harmonic space resolved spectra observed above in the lateral direction show a lumi-

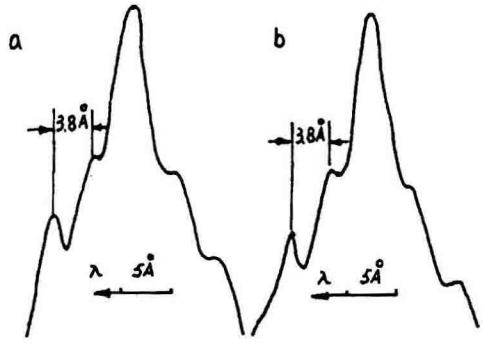

Fig. 5. $2\omega_0$ harmonic space resolved spectrum densitometric traces corresponding to fig. 4.

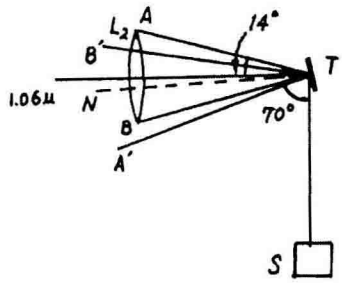

Fig. 6. Shooting diagram.

nescent length of 180 μm along the incident laser, which is consistent with the length (~180 μm) observed in the $2\omega_0$ harmonic time and space resolved structures in the same direction [13]. It is difficult to explain why the $2\omega_0$ harmonic emission displays such a large scale out of the critical surface according to the linear conversion theory based on the planar wave–plasma interaction [1,2,14]. First, the $2\omega_0$ harmonic emission could only be generated in the mirror-reflected direction of the incident laser [14], and its intensity is very weak in the normal incident case because the resonance absorption almost disappears [17]. In fact the incident angle is about 3° and the convergence angle of lens L_4 with respect to the target surface is 14° (see fig. 6) in our experiments. Therefore, the ray passing by the point A is reflected by the target surface, then forms an angle of 70° with respect to the direction perpendicular the incident laser. Thus, the intensity of the $2\omega_0$ harmonic emission in the lateral direction should be zero. Second, the $2\omega_0$ harmonic emission can only be generated near the critical surface and could not appear in a range of 180 μm out of the critical surface according to the planar wave–plasma interaction theory [1,2]. Finally, if the $2\omega_0$ harmonic emission resulted from the parametric decay [4] its spectrum should show a large red shift out of the critical surface, for example, the red shift of Al targets is in a range of 10–20 Å. But, the $2\omega_0$ harmonic space resolved spectra display, in our experiments, no red shifts within the whole luminescent region.

On the basis of the above discussion, it may be conceivable that the second harmonic emission observed in the lateral direction arises from the interaction of the laser beam with plasma filaments rather than the interaction of the planar wave with a plasma. In accordance with theory summarized in sect. 2, all

the above features can be explained. Because the narrow band laser irradiance on the target surface is non-uniform and it is easy to obtain plasma filaments, in which the fundamental wave has an asymmetric distribution about the filamentary axis; while the uniform illumination in the broad band irradiances makes the filamentation process difficult to generate, the $2\omega_0$ harmonic emission in the lateral direction is intense in the narrow band case and too weak to be observed in the broad band case.

It has been known that the laser irradiated plasma filaments extend outward from the critical surface [16], and there exists an intense radial field (the radial tunnel effect) at each point along the filamentary axis, which leads to the $2\omega_0$ harmonic generation. Therefore, the $2\omega_0$ harmonic luminescent region extends outward from the critical surface, the length of which is about equal to that of a plasma filament. On the other hand, it is the linear conversion of the $2\omega_0$ harmonic generation that we discuss in this paper. Furthermore, the spectrograph slit placed in the horizontal direction coincides with the filamentary axis so that a filament can be imaged on the slit. Therefore, the $2\omega_0$ harmonic space resolved spectrum could demonstrate a spectral line with a certain width and length (equal to the length of filaments), showing no spectral shifts.

Now, we begin to make further analyses of the interesting phenomena in the prepulse irradiance. Since a prepulse generates a large scale plasma corresponding to a lower density, a large part of the incident laser can arrive at the critical surface, causing the resonance absorption initiated by self-focusing filamentation described in ref. [17]. On the other hand, a radial tunnel effect also emerges, resulting in an intense local field at the radial resonance point [14]. These two effects all generate the linear conversion of the $2\omega_0$ harmonic emission so as to form an intense $2\omega_0$ harmonic region near the critical surface. However, the former effect will disappear out of the critical surface so that the $2\omega_0$ harmonic intensity becomes weak.

The emergence of the red and blue shifted peaks near the critical surface (fig. 4) arises from the wave vector limitation of the Langmuir wave in a modulated plasma [12]. Referring to ref. [12], one can express the wavelength difference between shifted peaks as

$$\Delta\lambda_2 = (4\lambda_2/\omega_2)\bar{k}(ZT_e/m_i)^{1/2}. \quad (1)$$

For the prepulse case, some nonlinear processes, such as two plasma decay and Raman scattering are produced in a larger scale filament. Thus the electron temperature rises, owing to the generation of a lot of superhot electrons in the nonlinear processes. When $T_e = 4$ keV [19], then $\Delta\lambda_2 = 3.6$ Å, close to the value of 3.8 Å measured in the experiments. Another important result caused by the plasma modulation is that the second harmonic space fringes can emerge near the critical surface [13]. If a prepulse generates an expanding plasma with a velocity of 0.42 cm/ns [20], the plasma characteristic length z_0 is $0.42 \times 1.5 = 6.3$ cm. Therefore, the fringe interval becomes 8.1 μm, calculated by the following formula

$$\Delta x = 1.5[z_0(\lambda_0/2\pi)^2]^{1/3}, \quad (2)$$

in agreement with that in the experiments. However, the fringe interval was calculated as $\Delta x = 4.4$ μm in the non-prepulse case [13]. These fringes bent either in or out with the time evolution [13]. As the space resolved spectra are integrated with respect to the time, one can not observe the clear space fringes in figs. 2 and 3.

Acknowledgements

We acknowledge valuable contributions to this work by Wang Guanzhi, Cheg Ruihua, He Xingfa, Bi Wuji, and Lin Kangchun and appreciate very much the assistance of the staff of the Six Laser Beam Facility.

Financial support of this work is from the Science Foundation of Academia Sinica under Contract No. R850957.

References

[1] N.S. Erokhin, S.S. Moiseev and V.V. Mukhin, Nucl. Fusion 14 (1974) 333.
[2] N.S. Erokhin, V.E. Zakharov and S.S. Moiseev, Sov. Phys. JETP 29 (1969) 101.
[3] V.P. Silin, Sov. Phys. JETP 21 (1965) 1127.
[4] J.L. Bobin, M. Decroisette, B. Meyer and Y. Vitel, Phys. Rev. Lett. 30 (1973) 594.

[5] M. Decroisette, B. Meyer and Y. Vitel, Phys. Lett. A 45 (1973) 443.
[6] N.G. Basov, V.Yu. Bychenkov, O.R. Rrokhin, M.V. Osipov, A.A. Rupasov, V.F. Silin, G.V. Sklizkov, A.N. Starodub, V.T. Tikhonchuk and A.S. Shikanov, Sov. J. QE 9 (1979) 1081.
[7] P.D. Carter and S.M.L. Sim, Optics Comm. 27 (1978) 423.
[8] A.G.M. Maaswinkel, Optics Comm. 35 (1980) 236.
[9] G. Auer, K. Sauer and K. Baumgärtel, Phys. Rev. Lett. 42 (1979) 1744.
[10] S. Jackel, S. Elliezer and A. Zigler, Phys. Rev. A 24 (1981) 1601.
[11] K. Tanaka, W. Seka, L.M. Goldman, M.C. Richardson, R.M. Short, J.M. Sourse and E.A. Williams, Phys. Fluids 27 (1984) 2187.
[12] Gu Min, Tan Wihan, Lin Zunqi, Bi Wuji, Yu. Wenyan and Deng Ximing, Phys. Fluids 30 (1987) 1515.
[13] Tan Weihan, Lin Zunqi, Gu Min, Shi Aing, Yu Wenyan and Deng Ximing, Phys. Fluids 30 (1987) 1510.
[14] Tan Weihan and Gu Min, Linear conversion theory on the second harmonic emission from a plasma filament, submitted to Phys. Fluids.
[15] M.J. Herbert, J.A. Stamper, R.R. Whitlock, R.H. Lehmberg and B.H. Ripin, Phys. Rev. Lett. 46 (1981) 328.
[16] Lin Zunqi, Tan Weihan, Gu Min, Mei Guang, Pan Chengming, Yu Wenyan and Deng Ximing, Laser Part. Beams 4 (1986) 223.
[17] Tan Weihan, Yu Wenyan, Lin Zunqi, Bi Wuji, Deng Ximing and Ding Liming, Laser Part. Beams 4 (1986) 231.
[18] Deng Ximing, Yu Wenyan, Chen Shisheng, Ding Liming and Tan Weihan, Acta Optica Sinica 3 (1983) 97.
[19] Guo Yongming, Ni Yuanlong, Wan Binggen, Gu Zhongmin, Wei Xiaochun and Tan Weihan, Chinese J. Lasers 14 (1987), in press.
[20] Tan Weihan, Lin Zunqi, Gu Min, Zhang Huihuang, Shi Aing, Yu Wenyan and Deng Ximing, Scientia Sinica A 30 (1987) 421.

THE MECHANISM FOR THE SECOND HARMONIC GENERATION IN LASER IRRADIATED MICROTUBE TARGETS

Wenhua CHEN, Min GU, Zunqi LIN, Wenyan YU, Weihan TAN and Ximing DENG
Shanghai Institute of Optics and Fine Mechanics, Academia Sinica, Shanghai, P.R. China

Received 15 February 1988

Reported in this paper are the $2\omega_0$ harmonic space and time resolved structures, observed at the back-scattering direction in laser irradiated microtube target experiments. The process of laser–microtube interaction has been analysed. According to the plasma filament interaction theory, primarily the special phenomena are explained of the back-scattering $2\omega_0$ harmonic emission within the microtube.

1. Introduction

Recently, a high population inversion between the 1s3p level and 1s4p level of He-like Mg^{+10} has been obtained, using a high power laser to irradiate microtube targets in the soft X-ray wavelength band [1].

Since the interaction of a laser with the microtube targets is rather sophisticated, it is necessary to use different diagnostic methods in our experiments. Presented here are the time and space resolved structures of the second harmonic emission observed in the back-scattering direction. By using the streak camera techniques, some interesting phenomena have been achieved. Analyzing these results, we can get a better understanding of the mechanism of the high population inversion.

2. Experiment arrangement

The experiments were carried out at the Six Beam Laser Facility in the Shanghai Institute of Optics and Fine Mechanics, Academia Sinica. The FWHM of the laser pulse with a spectral width of 0.2 Å was in the range of 100–250 ps. The output energy was 1–10 J, and the power density 5×10^{13}–3×10^{14} W/cm^2. The laser beam was focused by an aspherical lens L1 with a focusing spot of 60–80 μm (see fig. 1) on the microtube target surface.

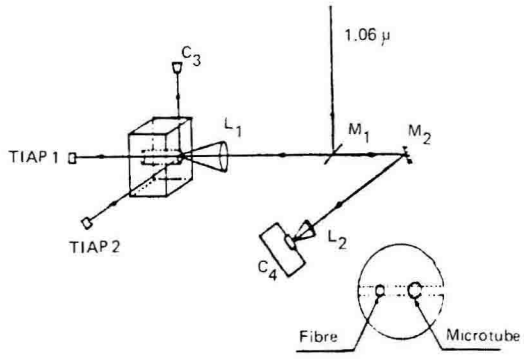

Fig. 1. The experimental setup.

Along and perpendicular to the microtube axis, two TLAP crystal spectrographes C1, C2, the main parameters of which were presented in ref. [2], were set. Thus, we can get resonant emission of the Mg ions inside and outside the microtube. Besides, there was a pinhole camera above the microtube.

The second harmonic emission of the plasma passing through an imaging system formed by ions L1 and a mirror M2 with wavelength of 0.53 μm was focused on the streak camera slit, which was adjusted to coincide with the diameter of the microtube.

In order to determine the mechanisms for the second harmonic emission, it is necessary to obtain the incident laser pulse profile. For this purpose, the laser pulse signal from the amplifier of the laser system was conducted to one end of the streak camera's slit,

0 030-4018/88/$03.50